Friction stir processing of AA6063-Ni particulate composite for fan exit guide vanes in high bypass ratio gas turbine engines

P. Anand Prabu[1] , Rajesh Jesudoss Hynes Navasingh[2,3], Muhammad Asad Ali[4],
Marian Bartoszuk[3*] , Nagarajan Jawahar Vignesh[5], N. Srinivasan[6]

[1] Department of Mechanical Engineering, VV College of Engineering, Tisaiyanvilai, Tirunelveli, Tamil Nadu, India
[2] Faculty of Mechanical Engineering Opole University of Technology, Proszkowska 76, 45-758 Opole, Poland
[3] Department of Mechanical Engineering, Mepco Schlenk Engineering College, Sivakasi, India
[4] Department of Industrial and Manufacturing Engineering, University of Engineering and Technology, Lahore 54890, Pakistan
[5] Department of Mechanical Engineering, SRM Madurai College for Engineering and Technology, India
[6] Department of Mechanical Engineering, Jansons Institute of Technology, Karumathampatti, Coimbatore - 641 659, Tamil Nadu, India
* Corresponding author's e-mail: m.bartoszuk@po.edu.pl

ABSTRACT

Fan exit guide vanes in high-bypass-ratio gas turbine engines reduce drag and increase efficiency. A significant quantity of more than 100 pieces of aluminium vanes are used in a gas turbine engine. By replacing aluminium with AA6063-Ni particulate composite vanes, it is possible to achieve a notable weight reduction per engine. In the present work, the friction stir processing (FSP) technique is employed for the development of develop AA6063-Ni particulate composite. The AA6063 matrix is lightweight with high strength and better extrudability applications, whereas the reinforcement metal (nickel) has high resistance to corrosion, toughness, and high impedance. The specimens are made with a groove of depth 4.5 mm and width of three variable dimensions, such as 0.4 mm, 0.8 mm, and 1.2 mm. It is processed effectively by combining a lower travel speed of 20–40 mm/min with a tool rotating speed of 1200–1500 rpm. The results showed that Ni particles were uniformly dispersed with a remarkable grain refinement, which enhanced hardness by 35% and made the composite suitable for aerospace applications.

Keywords: friction stir welding, mechanical properties, scanning electron microscopy.

INTRODUCTION

Currently every sector is attempting to minimise component weight while increasing specific strength. Aluminium matrix composites (AMCs) meet the need for novel materials development. Ceramic particles are frequently used to strengthen AMCs [1, 2]. Because of their low cost and strong wettability with molten aluminium, SiC and Al_2O_3 were frequently utilised as reinforcing phases [3].

As a solid-state method for developing surface and bulk AMCs, friction stir processing (FSP) has recently drawn much scientific interest [4, 5]. A new solid-state joining technique, FSP is founded on the ideas of friction stir welding (FSW), which was initially developed for aluminium alloys [4]. Using grooves of varying profiles, the ceramic particles are initially compressed along the traverse direction of the tool. FSP causes significant plastic deformation in the aluminium alloy, allowing the crushed ceramic particles to be mixed into the matrix with the help of the violent stirring action of the spinning tool. The composite is developed and consolidated due to the tool movement and the applied axial force, whereas particle kind,

size, and shape have no significant impact on the FSP process [6–8]. FSP can improve material mechanical characteristics by removing casting imperfections locally by refining microstructures [9]. In situ composites made of aluminium offer several benefits over their traditional equivalents. FSP can be used to efficiently homogenize the particle dispersion in situ composites made of aluminium. [10,11]. Friction-based processing procedures include coating of ceramic slurry in the interface that acts a heat buffer zone that prevents excessive heat and also helps in dispersion [12, 13]. Buffer interlayers of pure metals or coating are also used in friction-based processing methods. They are found to enhance joint strength [14].

A high-bypass-ratio gas turbine engine's fan exit guide vanes (FEGV) made of 108 aluminium parts increase efficiency and decrease drag. A weight saving of approximately 50 lb per engine is still possible by using AA6063-NiParticulate Composite vanes in place of aluminium vanes [15]. A metal particle reinforced composite was developed by embedding nickel particles into an Al matrix using FSP. FSP produced significant matrix grain refinement, uniform nickel particle dispersion, and strong bonding in the interfacial region of Al matrix. The yield strength has increased thrice while considerable ductility has been preserved. The hardness has also significantly enhanced [16]. Ishi and McNelley [17] employed optical microscopy (OM) and transmission electron microscopy (TEM) techniques to examine the impact of FSP parameters on the evolved microstructure in an equilibrium-cooled, NiAl bronze alloy. Using a threaded pin tool with adjustable traversal and tool rotation speeds, the longitudinal variation of stir zone microstructures to FSP parameters was examined. Their results show that in contrast to the processing at lower rotation and traversal rates, processing at higher rates results in steeper temperature gradients and higher peak temperatures near the surface of the tool.

Using FSP, Qian et al. [18] made in situ synthesised Al_3Ni composites by incorporating Ni powder into the stirred zone of the aluminium alloy. The microstructures and compositions of the composites were investigated using SEM, EDS and XRD. The ultimate tensile strength (UTS) and micro-hardness of the material were assessed. Al_3Ni was the result of the in-situ mixture, as determined by XRD and EDS studies, and subsequently, the effective Gibbs free energy change of

formation model was proposed at the solid-state interface. According to Giles et al. [19], friction stir processing improves and homogenises the microstructure resulting in increases of ductility and fracture resistance in processing aluminium lithium alloy. OM and TEM techniques with orientation imaging microscopy were utilised in order to analyse the microstructure of the material that had been subjected to FSP. Ke et al. [20] employed FSP to make bulk Al–Ni intermetallic composites with Ni reinforcement. The hardness and tensile characteristics were measured, as well as the microstructures were observed with the compositions. It was successful in producing Al_3Ni composites.

Machine and tool parameters, and material attributes are to be considered in FSP (Figure 1). The processing conditions in FSP are selected based on the yield strength, ductility, and hardness of the base material, since they influence plastic deformation, according to Sharma et al. [21]. Tool traverse speed and tool rotation rate are two important machine variables. The rotation-transverse speeds of the tool determine the amount of heat generated in the processed material, which influences microstructure and characteristics. Shoulder (diameter and feature) and probe (form, size, and feature) are all part of tool geometry. Proper cooling arrangements can result in nano-sized grains. The added benefit of cooling during FSP is that it reduces tool wear [21].

Metal matrix composites have been made possible in a variety of various industries, including automobile transport and railways, aerospace, and industrial applications because of their functional properties (structural efficiency, wear resistance) as well as appealing thermal properties and electrical characteristics. Some difficult technological difficulties have been addressed, including cost-effective processing, various approaches to material design and development, as well as the characterisation and management of interfacial properties [22]. AA6063 alloys are commonly utilised in the construction of boats and ships. Erosion corrosion can occur on a moving aluminium alloy ship in seawater. The increased corrosion assault on metals caused by the relative motion of corrosive fluid is known as erosion-corrosion. As a result, an increase in the erosion corrosion resistance of an aluminium alloy is required. By integrating both artificial and natural aging processes, greater erosion-corrosion resistance was achieved [23].
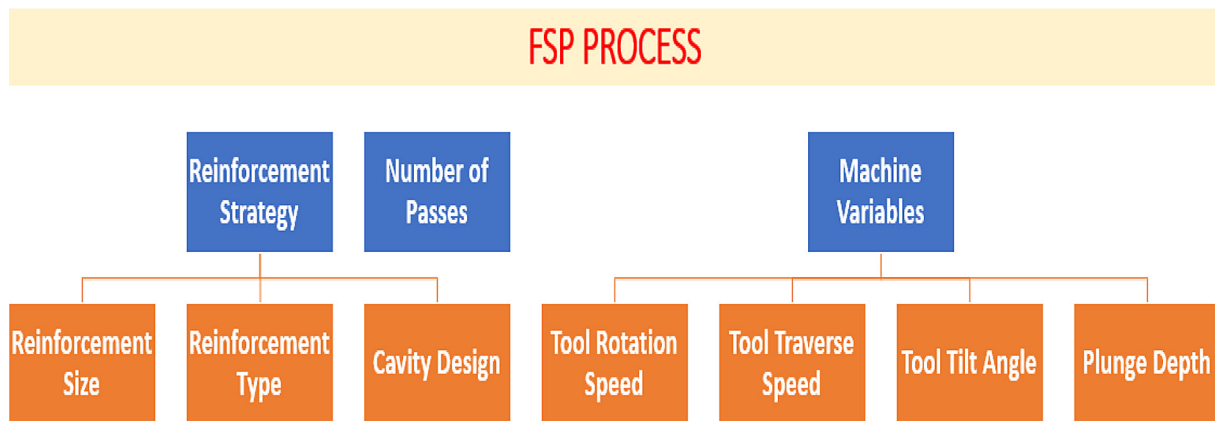
FSP PROCESS

Figure 1. Classification of key FSP process variables

Friction stir processing of AA6063-Ni particulate composite is carried out in the current study using a friction stir welding equipment. To determine its appropriateness for the application, microstructural features were assessed.

MATERIALS AND METHOD

Workpiece

The workpiece was cut into certain segments of specific dimensions, 150 × 50 × 10 mm. The AA6063 bar was cut into six pieces. Then, to fill the reinforcement material a groove was made on the surface of the AA6063 bar. The width of the groove is made a different dimension as 0.4 × 0.8 × 1.2 mm with groove depth 4.5 mm. AA6063 composition as well as properties of AA6063 and Ni powder are given in Tables 1–3, respectively.

The microstructural image of the reinforcement material, i.e., Nickel powder, is analysed using the SEM, and microstructural images (Figure 2) are viewed in the magnifications of ×700, ×2000, ×5000, and ×10000. The particle size analysis is made based on the microstructural images of the SEM instrument; from that, it can be

understood that the size of Ni is from 35 to 110 μm and is spherical in shape. This detail confirms that particle size is probably uniform and spherical.

Tool design and materials

The tools used in friction stir processing are classified into pin tools and pinless tools. These are classified based on machining comfort. The tool comprises HCHCr steel (high carbon high chromium steel). This kind of alloy steel is used for fabricating the composite because it has good strength, high resistance to corrosion, and negligible deformation while fabricating the composite at a very high load and high withstanding capacity towards temperature.

EXPERIMENTAL SETUP

The specimens are made with the dimensions 150 × 50 × 10 mm. The grooves of various widths are made on each specimen. A pair of specimens are grooved with the widths of 0.4 mm, 0.8 mm and 1.2 mm. They are made using the wire-cut electric discharge machining (WEDM). This

Table 1. Chemical composition of AA6063

Mg	Si	Mn	Zn	Ti	Cu	Fe	Cr	Al
0.75%	0.45%	0.10%	0.10%	0.10%	0.10%	0.35%	0.10%	Balance

Table 2. Physical properties of AA6063

Density	Melting point	Thermal expansion	Modulus of elasticity	Thermal conductivity	Hardness (Rockwell)
2.70 g/cm^3	655 °C	23.5 x10^{-6}/K	69.5 GPa	201 W/mK	35.5 HR

Table 3. Physical properties of Ni

Density	Melting point	Boiling point	Thermal conductivity	Electrical resistivity	Youngs' modulus	Poisson ratio	Hardness (Vicker)
8.908 g/cm^3	1728 K	3003 K	90.9 W/mK	69.3 nΩm	200 GPa	0.31	638 MPa
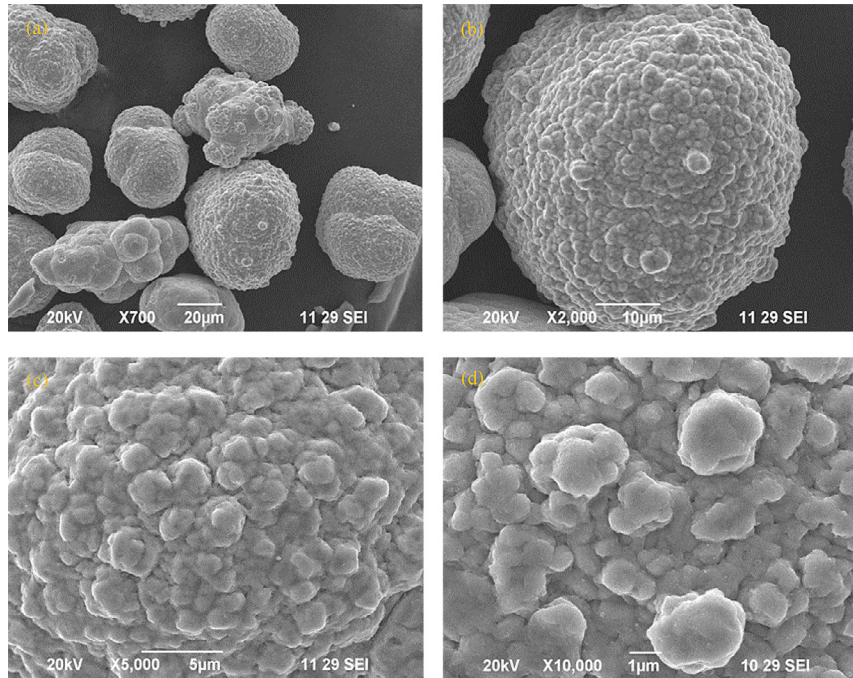
Figure 2. SEM of Ni powder at magnifications; (a) ×700, (b) ×2000, (c) ×5000, (d) ×10000

method of machining is preferred because the accuracy and the surface finish of the groove are perfect. At first, the grooved specimen is taken, and any damage on the surface, except the grooved area, could be removed by using the grinding process. Most probably the damages will be in the form of any rust or other impurities on the surface of AA6063. The sides of the groove are closed by using a nail and a hammer, by hitting the sides, the groove side openings are closed. The powder nickel is placed in the grooved area. The powdered material is inserted well in the grooved area by using gauges to ascertain thicknesses. After filling the nickel powder inside the grooved area, the specimen is ready for FSP. The recommended parameters for the FSP are fed into the friction stir welding machine. The specification of FSP machine is FSW 30–300 (30 kN, 3000 rpm).

FSP is done to all the specimens of the groove 0.4 × 0.8 × 1.2 mm with the specified parameters for carrying out the process. After all the arrangements are made, FSP is first done with the pin-less tool. This is done to close the grooved. The grooved area is closed to stop the dropping of reinforcement from the groove due to the rotating force of the tool. Once the process is done with the pin-less tool, then, the process with the pin tool is done. The pin tool is plunged into the workpiece surface, and then rotated at a specific speed, specific feed rate, and specific load. Finally, the composite is fabricated. The experimental illustration of the FSP process for the composite fabrication is presented in Figure 3. Macrostructural analysis, and hardness tests were subsequently carried out using the test coupons. Figure 4(a, b) shows the specimen polishing and hardness testing. The processing parameters for the fabrication of composites using FSP, such as Feed rate, Speed, and Load, are given in Table 4.

Volume fraction

The volume fraction of nickel in the aluminium composites is based on area of pin and groove area. There are three kinds of grooves widths (0.4, 0.8, 1.2 mm) used in this work. On the basis of these widths, four different kinds of volume fractions of Ni (i.e., four kinds of groove areas)
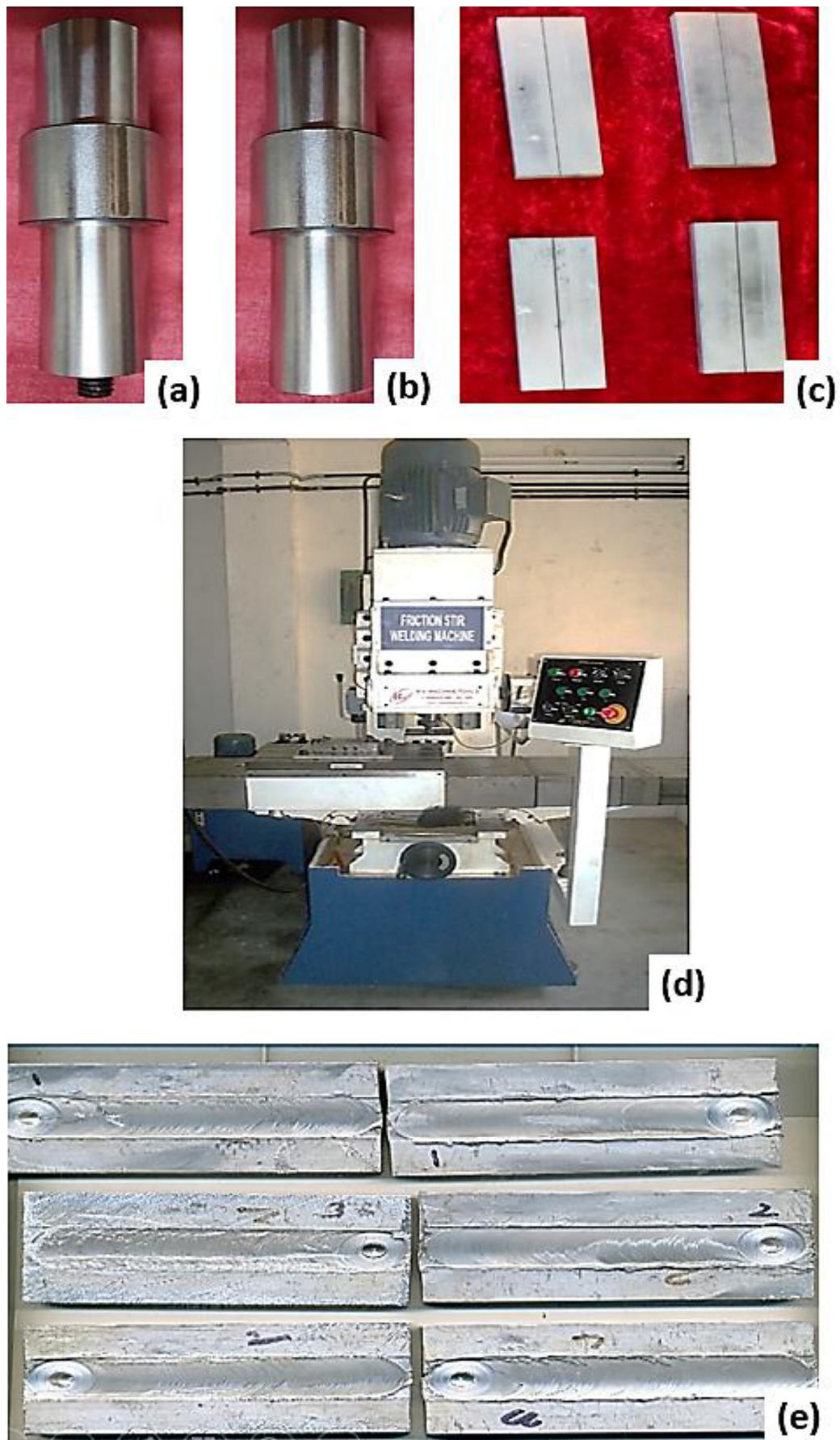
Figure 3. Experimentation illustrations: (a) pin tool (b) pin-less tool (c) grooved AA6063 specimens
(d) friction stir welding machine (e) specimens of FSPed composite
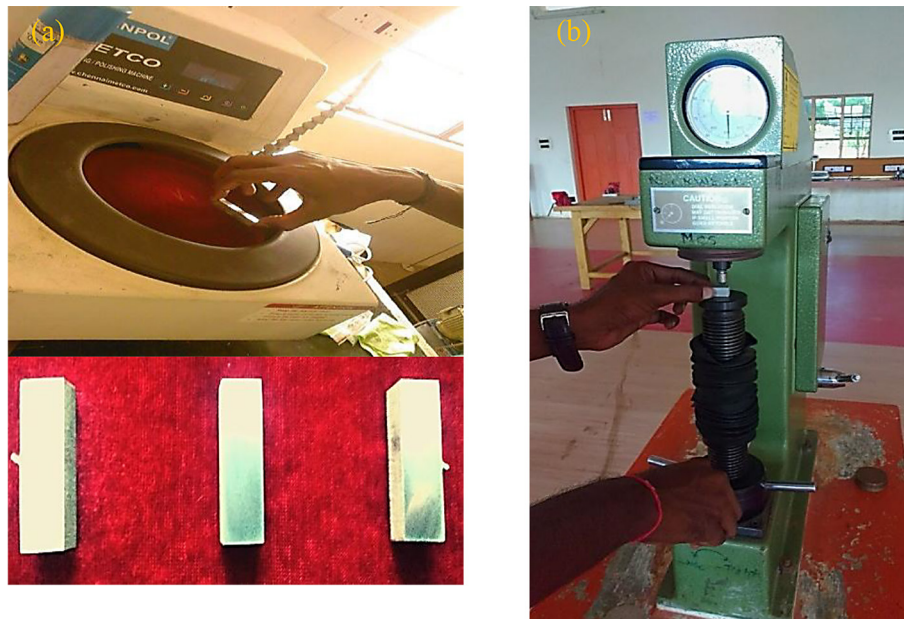
Figure 4. (a) Specimens polishing, (b) hardness testing

Table 4. Process parameters for welding experiments

Parameters	FSP with Pinless tool	FSP with Pin tool
Spindle speed	1200 rpm	1500 rpm
Feed rate	40 mm/min	20 mm/min
Axial Load	12 kN	12 kN
Dwell time	6 s	6 s
Rotation direction	Clockwise	Clockwise
FSW control	Vertical direction	Vertical direction

were obtained. The area of the pin cross section is almost constant. In each case the percentage of nickel in aluminium composites was doubled when compared to previous one. Table 5 gives the volume fraction of nickel in aluminium composites prepared during the processing.

RESULTS AND DISCUSSION

Macro structural analysis

From the plates, the cross-section of FSPed aluminium composites is shown (Figure 5). The FSPed zones are free from any tunnels and holes. The process parametric settings used in this study are sufficient to generate enough frictional heat to plasticise AA6063/5.45 wt.% of Ni, AA6063/10.9 wt.% of Ni, and AA6063/16.36 wt.% Ni.

To determine the possible working limits of the FSW process, a significant number of experimental trials were done on 6 mm plates of
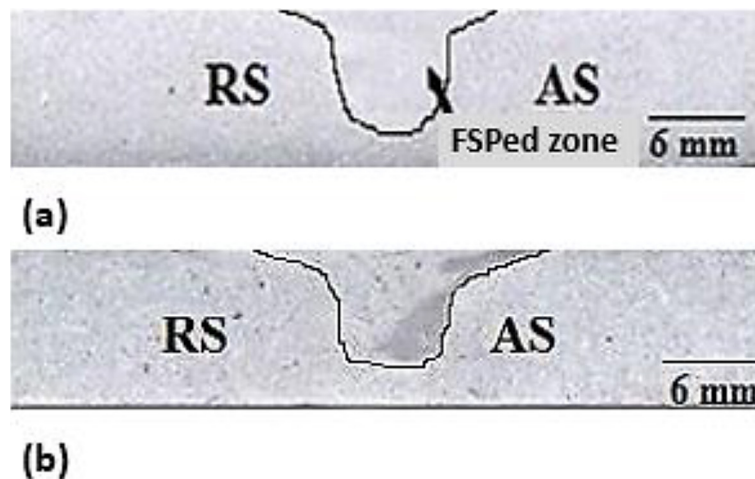
AA6063Ni composites by varying one of the parameters while the others were kept constant. All of the joints used in this study were examined using an optical microscope to determine the quality of the FSP areas. The operating range of each process parameter was determined by analysing the absence of obvious flaws such as tunnel faults, pinholes, and so on. Depending on the welding speed, a rotating speed of 700 to 1600 r/min produced defect-free joints, with welding feed rates ranging from 30 to 150 mm/min. The macrostructures of the joints manufactured employing welding rates of 30–150 mm/min and rotating speeds of 500 to 300 r/min as similar way in another study [24].

Microstructural analysis

The microstructure of the composites was analysed using an optical microscope at the magnification range of 150X. Microstructural analysis

Table 5. Volume fraction of nickel% in composite

Pin diameter	Pin length	Groove width	Groove depth	Cross sectional area of pin	Area of groove	Volume fraction
mm				(mm)^2		%
6	5.5	0	0	33	0	0
6	5.5	0.4	4.5	33	1.8	5.45
6	5.5	0.8	4.5	33	3.6	10.91
6	5.5	1.2	4.5	33	5.4	16.36

Figure 5. Cross section of microstructure of FSPed composites; (a) AA6063/5.45 wt.% Ni, (b) AA6063/10.9 wt.% Ni

revealed fine and equiaxed grains in the stir zone (SZ), as well as the role of nickel particles as heterogeneous nucleation sites in the dynamic recrystallization of Al grains. The microstructure of a friction stir weld may be divided into three distinct areas. The stir zone, the thermomechanically affected zone, and the heat impacted zone are the three zones. Figure 6(a) shows the optical photomicrograph of the base Aluminium metal. Magnified view of boundary region of FSPed zone is shown in Figure 6(b). Figures 6(c-e) show the optical micrograph of FSPed zones of plasticised AA6063/5.45 wt.% Ni, AA6063/10.91 wt.% Ni, AA6063/16.36 wt.% Ni respectively. Figure 6 shows the distribution of nickel particles. Furthermore, no particle aggregation was found, and the particles had uniform dispersion.

Optical microphotographs display a uniform distribution of nickel particles (Figure 6). Defect-free stir zones indicate that material is flowing efficiently around the pin tools. SZ is normally the same size as the revolving pin, measuring 6 mm in diameter and 5.5 mm in length. Due to the presence of intense swirling throughout the procedure, the nickel particles were observed to be spread inside

this area. There are no noticeable flaws in the interface zone, and the surface composite layer looks to be firmly attached to the Al substrate. Within the stir zone, severe plastic deformation and frictional heating result in the development of a recrystallized fine grains. In the aluminium matrix, there is no distinct clustering of particles. The average size of nickel particles observed as 20–24 μm in FSP zones. This is due to the vigorous swirling and mixing of the material during FSP, which caused the coarse nickel particles and dendritic structure to break apart, resulting in a homogenous distribution of finer Nickel particulates throughout the AA6063/Nickel composites. Significant reinforcing particle disintegration in the SZ has been documented as the result of strong plastic deformation. The interface is firmly attached to the matrix, with no voids or other flaws visible in the images. All of the other developed samples exhibited a similar interface as reported [25].

Hardness test

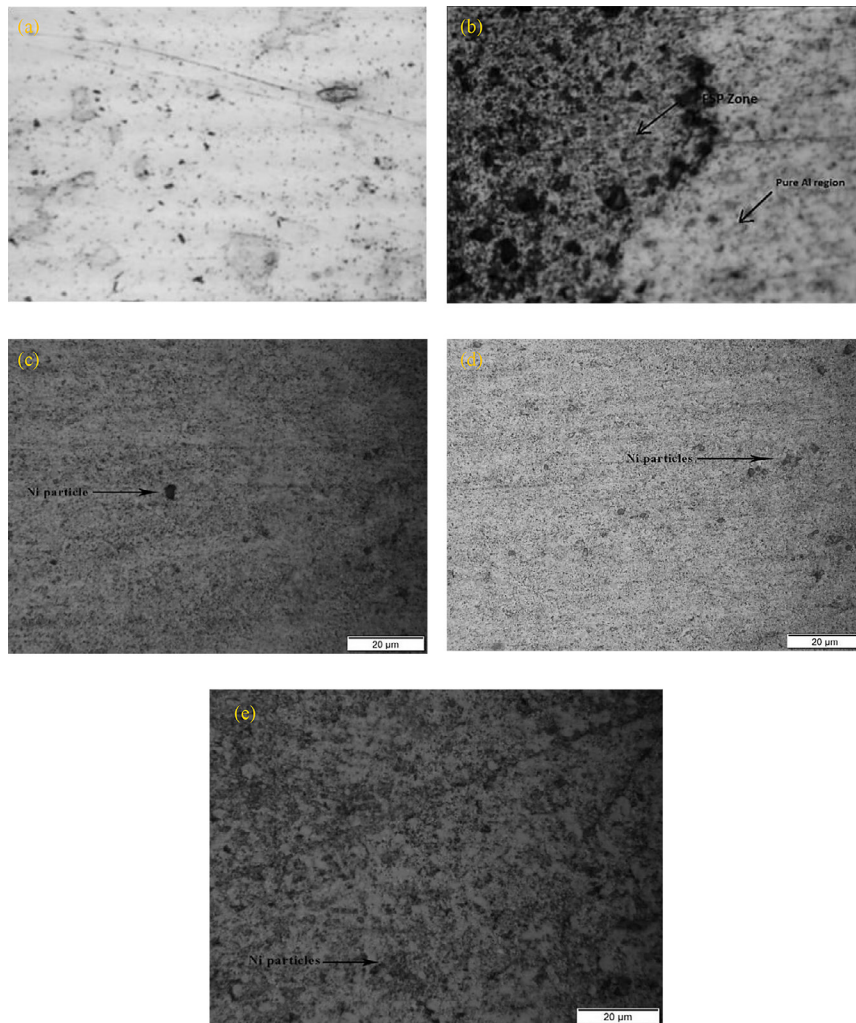From Figure 7, it can be observed there is a gradual increase in hardness for 0–5.5 wt.% of

Figure 6. Microstructural images (a) base metal AA6063, (b) boundary region,
(c) FSPed zone of AA6063/5.45 wt.% Ni, (d) FSPed zone of AA6063/10.9 wt.% Ni,
(e) FSPed zone of AA6063/16.4 wt.% Ni

nickel in AA6063 and a sudden increase of 5.5–16.4 wt.% of nickel in AA6063. It is clear that when the volume of nickel in AA6063 in the composite is increased, the hardness level of the composite also increases up to a particular then there will be decrease in hardness upon further addition of nickel powder in AA6063. Therefore, for the particular amount of nickel (up to 6–20) addition improves the hardness. Thereafter, it will reduce the hardness. One of the most important things that is found in this experiment is that the reinforcement material size is broken or reduced due to FSP. This results in an increase in the smaller grain size of reinforced material that improves the mechanical properties of the composite by using FSP-similar behaviour reported in other studies [26, 27] (Table 6).

The issues related to the machining of gas turbine blades stem directly from their manufacturing process and the shape of the blank. It should

be noted, however, that the blade shape determines the shape of the blank and, consequently, the entire manufacturing process. Therefore, to optimally design the manufacturing process as a whole, it seems advisable to use the tools that combine knowledge from machining, materials engineering, and, importantly, flow mechanics. A case in point is publication [28], which describes the importance of fluid dynamics and boundary layers for airflow. For this reason, further research should strive to combine these three areas of knowledge into a single, coherent approach.

CONCLUSIONS

Development of AA6063-Ni composite with different volume fractions of Ni powder (5.45%, 10.9% and 16.36%) was successfully achieved,
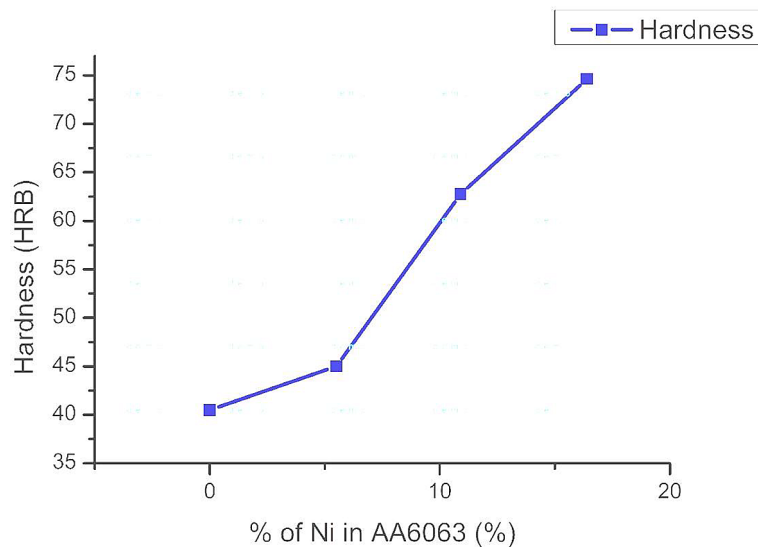
Figure 7. Average hardness value vs. wt.% of Ni in AA6063

Table 6. Hardness testing results

Specimens	P 1	P 2	P 3	P4	HRB
AA6063	37.5	40	41.5	43	40.5
AA6063/5.45 wt.% Ni	43	47	51	39	45
AA6063/10.9 wt.% Ni	58	67	65	61	62.5
AA6063/16.4 wt.% Ni	73	77.5	76	72	74.625

and the micro-harness and microstructural analysis were carried out. The microstructural analyses that are made on the composite are SEM and Optical Microscopy. Because of the pinning action of the Ni particle, the grain size of the stir zone with Ni particles was lower than that of the Stir Zone without Ni particles. Because of the enhanced microstructure, hardness improved dramatically following FSP. Due to the changes, breaking up, and homogeneity of Ni particles, hardness increased in the stir zone (SZ), according to the observations. The uniform dispersion of Ni particles, which have extraordinarily high hardness, as well as considerable microstructural alterations caused by FSP, are thought to have resulted in an increase in hardness. Because of the smaller grain of reinforcing Ni particles on the aluminium matrix, the micro-hardness of the SZ with Ni particles was greater than that of the SZ without Ni particles. In AA6063/16.36 wt.% Ni from the matrix metal, the hardness increased by 35%.

The future directions for studies include improving mechanical performance under dynamic and fatigue loads, optimisation of process parameters using machine learning and improved corrosion resistance for aerospace applications. Finite element analysis, molecular dynamics simulations, and other computational modelling approaches can assist predicting outcomes and optimizing fabrication pathways. Real-world applications will depend on exploring alternative reinforcements and hybrid composites, scaling up manufacturing methods, and evaluating industrial feasibility.

REFERENCES

1. Sundar G., Rajesh N.J.H. Reinforcement in aluminium metal matrix composites. AIP Conf. Proc. 29 August 2019; 2142(1): 070006. https://doi.org/10.1063/1.5122398

2. Hynes N.R.J., Raja S., Tharmaraj R. et al. Mechanical and tribological characteristics of boron carbide reinforcement of AA6061 matrix composite. J Braz. Soc. Mech. Sci. Eng. 2020; 42: 155. https://doi.org/10.1007/s40430-020-2237-2

3. Yigezu B.S., Jha P.K., and Mahapatra M., The key attributes of synthesizing ceramic particulate reinforced Al-based matrix composites through stir casting process: a review. Materials and Manufacturing Processes, 2013; 28(9): 969–979.

4. Ma Z., Friction stir processing technology: a review. Metallurgical and materials Transactions A, 2008; 39(3): 642–658.

5. Arora H., Singh H., and Dhindaw B., Composite fabrication using friction stir processing—a review. The International Journal of Advanced Manufacturing Technology, 2012; 61(9): 1043–1055.

6. Tharmaraj R., Hynes N., and Velu P.S., Investigation on friction stud welded AMC/AISI 304 steel joints with ceramic intercoating. Journal of the Brazilian Society of Mechanical Sciences and Engineering, 2020. 42(10): 1–8.

7. Sahraeinejad S., et al., Fabrication of metal matrix composites by friction stir processing with different particles and processing parameters. Materials Science and Engineering: A, 2015; 626: 505–513.

8. Dinaharan I., Influence of ceramic particulate type on microstructure and tensile strength of aluminum matrix composites produced using friction stir processing. Journal of Asian Ceramic Societies, 2016; 4(2): 209–218.

9. Bauri R., Yadav D., and Suhas G., Effect of friction stir processing (FSP) on microstructure and properties of Al–TiC in situ composite. Materials Science and Engineering: A, 2011; 528(13–14): 4732–4739.

10. Karthikeyan L., et al., Mechanical property and microstructural changes during friction stir processing of cast aluminum 2285 alloy. Materials & Design, 2009; 30(6): 2237–2242.

11. Hynes N.R.J., et al. Numerical investigation on friction welding of alumina/AA 6063 T6 joints. in AIP Conference Proceedings. 2016. AIP Publishing LLC.

12. Hynes N.R.J., Prabhu M.V., and Nagaraj P., Joining of hybrid AA6063-6SiCp-3Grp composite and AISI 1030 steel by friction welding. Defence technology, 2017; 13(5): 338–345.

13. Velu, P.S., Hynes N.R.J., and Vignesh N.J., Joining of AA 6061/Ti–6Al–4V with zinc interlayer using friction welding process. Journal of the Brazilian Society of Mechanical Sciences and Engineering, 2019; 41(12): 1–13.

14. Hynes N.R.J., Sujana J.A.J., and Karuppasamy P., Simulation of friction stud welding process with an inter-metallic layer. International Journal of Applied Engineering Research, 2014; 9(26): 9028–9030.

15. Blecherman S. and Stankunas T., Composite fan exit guide vanes for high bypass ratio gas turbine engines. Journal of Aircraft, 1982; 19(12): 1032–1037.

16. Yadav D. and Bauri R., Processing, microstructure and mechanical properties of nickel particles embedded aluminium matrix composite. Materials Science and Engineering: A, 2011; 528(3): 1326–1333.

17. Oh-Ishi K. and McNelley T.R., The influence of friction stir processing parameters on microstructure of as-cast NiAl bronze. Metallurgical and Materials transactions A, 2005; 36(6): 1575–1585.

18. Qian J., et al., In situ synthesizing Al_3Ni for fabrication of intermetallic-reinforced aluminum alloy composites by friction stir processing. Materials Science and Engineering: A, 2012; 550: 279–285.

19. Giles T.L., et al., The effect of friction stir processing on the microstructure and mechanical properties of an aluminum lithium alloy. Metallurgical and Materials Transactions A, 2009; 40(1): 104–115.

20. Ke L., et al., Al–Ni intermetallic composites produced in situ by friction stir processing. Journal of Alloys and Compounds, 2010; 503(2): 494–499.

21. Sharma, V., U. Prakash, and B.M. Kumar, Surface composites by friction stir processing: A review. Journal of Materials Processing Technology, 2015; 224: 117–134.

22. Miracle D., Metal matrix composites–from science to technological significance. Composites science and technology, 2005; 65(15–16): 2526–2540.

23. Pratikno H., Aging treatment to increase the erosion-corrosion resistance of AA6063 alloys for marine application. Procedia Earth and Planetary Science, 2015; 14: 41–46.

24. Vignesh N. J., Shenbaga Velu P., et.al. Enhancing AA5083/MGAZ31B Properties Via Friction Stir Welding, Surface Review and Letters, 2024, https://doi.org/10.1142/S0218625X24501282

25. Rajakumar S., Muralidharan C., and Balasubramanian V., Establishing empirical relationships to predict grain size and tensile strength of friction stir welded AA 6061-T6 aluminium alloy joints. Transactions of Nonferrous Metals Society of China, 2010; 20(10): 1863–1872.

26. Hynes N.R.J, Vivek Prabhu, M., et al., An experimental insight of friction stir welding of dissimilar AA 6061/Mg AZ 31 B joints. Proceedings of the Institution of Mechanical Engineers, Part B: Journal of Engineering Manufacture, 2022; 236(6–7): 787–797.

27. Vivek Prabhu M., Hynes N.R.J., Varun Kumar B., Aathi J. Numerical investigation of heat transfer in friction stir welding of Al/Mg joints. AIP Conference Proceedings, 2024; 3160, 060002. https://doi.org/10.1063/5.0225251

28. Oleksii Lanets O., Dmytriv T. Mathematical model of the boundary layer of airflow over a flat surface, Ujmems, 2025, 11/1, 28–36. https://doi.org/10.23939/ujmems2025.01.028